CONFIRMING DRY-SEASON GREEN-UP IN CENTRAL AMAZON FORESTS WITH LANDSAT 8 AND THE ROLE OF LEAF DEMOGRAPHY IN MODIS-MAIAC SEASONAL SPECTRAL PATTERNS

Nathan Borges Gonçalves [1,5], Aline Pontes Lopes [2], Ricardo Dalagnol [3], Jin Wu[4], Bruce Walker Nelson [5]

[1]Michigan State University, Department of Forestry, College of Agriculture & Natural Resources, East Lansing, MI, USA, nathanborges@gmail.com; [2]INPE – National Institute for Space Research, São José dos Campos, SP, alineplopes@gmail.com; [3]INPE, ricds@hotmail.com; [4]University of Hong Kong, School of Biological Sciences, jinwu@hku.hk; [5]INPA – National Institute for Amazon Research, Manaus, AM, bnelsonbr@gmail.com

ABSTRACT

We ask: (Q1) For two Central Amazon forest regions, do Landsat 8 OLI seasonal patterns of Green chromatic coordinate (Gcc), EVI and NIR corroborate BRDF-corrected Modis-MAIAC? (Q2) What are the biological drivers of Modis-MAIAC EVI and Gcc seasonality? For Q1 we obtained, for two Landsat 8 scenes, seasonal image sets having minimal difference in their artifacts from sun-sensor geometry. We found seasonal patterns for both spectral indices and for NIR from Landsat 8 were consistent with local Modis-MAIAC, thus confirming Modis detections of dry season green-up. For Q2, we found the fraction of upper canopy crowns with young leaves (< 1mo) was highly correlated with Modis-MAIAC Gcc. The fraction of crowns with mature leaves (2-7 mo) was highly correlated with Modis-MAIAC EVI. LAI, estimated by two methods, was poorly correlated with seasonal spectral changes.

Keywords — *tropical forest green-up, EVI seasonality, phenocam, leaf demography, LAI*

1. INTRODUCTION

Flux tower data suggest that evergreen central Amazon forests increase their photosynthetic capacity and photosynthesis (GPP) after accelerated leaf turnover (green-up) in the dry season and that leaf demography effects on canopy spectra are detectable in Modis Enhanced Vegetation Index (EVI) [1,2]. However, questions have been raised regarding the detection of seasonal and interannual forest spectral patterns [3,4]. Sun-sensor geometry, cloud contamination and topographic shadow contribute seasonal artifacts. Improved cloud filtering and BRDF correction in the Modis-MAIAC product apparently resolved these problems [5,6].

The biology driving the Modis spectral signal remains poorly investigated, though a landmark study at an East-Central Amazon site [7], using radiative transfer models driven by leaf-level spectral changes with age, reported recently that seasonal EVI pattern is mainly controlled by large seasonal change in leaf age, not by leaf amount, nor by

seasonal changes in climate. Nonetheless, few studies compare seasonal vegetation indices from Modis-MAIAC to (i) indices from higher resolution orbital sensors or to (ii) upper canopy leaf demography from tower-mounted RGB cameras. These are necessary to confirm and explain seasonal and interannual spectral patterns of Modis-MAIAC.

Here we first test the reliability of Modis-MAIAC BRDF correction and cloud filter for detecting seasonal changes in vegetation indices of Central Amazon forest canopies. To this end, we seek corroboration from Landsat 8 OLI (L8) of the MAIAC seasonal ranking for each index across two dates in one L8 scene and across three dates in a second scene. L8 image sets in each scene were chosen for (i) clear seasonal contrast of Modis-MAIAC vegetation indices and (ii) small or nil differences in L8 sun-sensor geometry artifact. L8 also has a 30m spatial resolution that permits reliable cloud filtering.

We extracted two vegetation indices from both L8 and Modis-MAIAC: EVI and Gcc (Green chromatic coordinate). Tower-mounted phenocams show that Gcc is useful for detecting recently flushed crowns in evergreen tropical forest [6,8] and thus also useful for estimating monthly leaf age mix of the upper canopy. After corroborating the Modis-MAIC seasonal spectral signals with L8, we used tower-mounted cameras at two additional Central Amazon sites to investigate how leaf demography is related to seasonal changes in Modis-MAIAC EVI and Gcc.

Our specific objectives are expressed as two questions, given in the Abstract.

2. METHODS

At the core of the debate over Modis detection of Amazon forest dry-season green-up using EVI is the sun-sensor geometry artifact. According to Morton *et al*. [4], this alone fully explains the increase in EVI during the drier months in the Central Amazon. They used Modis collection 5 data from Terra and Aqua platforms. Indeed, solar zenith angle of Modis for a pixel at nadir view decreases by about 15º in the Central Amazon from June to November. This reduces within-pixel shadow associated with irregularity of canopy and of underlying landforms, with consequent increase in

reflectance of the near infrared band, which is the main driver of EVI change [3].

To avoid these pitfalls, a simple solution takes advantage of the fact that the same solar zenith angle repeats up to four times per year near the equator, at the fixed hour of Landsat overflight [9]. We used two methods to eliminate sun-sensor geometry effects when comparing vegetation indices from different seasons in the same L8 scene. When the seasonal difference between solar zenith angles (SZA) of two images was < 0.7°, BRDF differences were assumed to be nil for upland forest pixels located < 0.5° off-nadir [9]. A suitable pair of images for this method was found for scene 230/61, centered 225 km NE of Manaus and 90 km NNE of the Amazon Tall Tower (ATTO):

- late wet season (15 May 2015), L8 SZA 33.00°;
- early wet season (09 Dec 2015), L8 SZA 32.44°;

When the SZA differed by 0.7°-4.0°, we controlled for BRDF as a covariable, represented by the phase angle. This is the angle between the solar illumination vector and the sensor view vector of a pixel [5]. The phase angle combines into one variable the main components of sun-sensor geometry effects on a pixel's reflectance [10]. The calculation is:

Phase angle = ACOS(cos(sensor view Zen)×cos(Sun Zen))+(SIN(sensor view Zen)×SIN(Sun Zen)*COS(Relative Azim angle)).

We obtained L8 Gcc and EVI from different seasons for cloud-free pixels having similar phase angles, using the entire L8 scene area. To obtain pixel sets with similar phase angle, we grouped pixels into narrow bins of phase angle and calculated the mean and the CI of the spectral index for each bin at each date. We did this for three image dates of L8 scene 230/63 centered 160 km south-southeast of Manaus city:

- mid-wet season, 11 Feb 2016, DOY 48, SZA 32.15°;
- wet-dry transition, 25 May 2013, DOY 144, SZA 36.18°;
- dry season, 02 Aug 2015, DOY 224, SZA 36.13°.

All five L8 images were in units of surface reflectance, the Level 2 product from Earth Explorer-USGS. We masked clouds and their shadows in Landsat using an adaptation of the Multi-temporal Cloud Masking (MCM) method [11]. We used only pixels of intact forest on flat upland. We excluded rivers, streams, floodplains, bottomlands and slopes. To this end, we processed SRTM to mask all Landsat pixels having (i) less than 15m Vertical Distance to Channel Network [12] or (ii) slope > 4°. The latter masks topographic shadows that shift position with the changing solar azimuth. We used PRODES data [13] to mask deforestation in both Modis and L8. We used 1-km resolution HAND (Height Above Nearest Drainage) [14] to mask rivers, streams and seasonally flooded areas in Modis.

The partially processed 1-km Modis-MAIAC product is available at 16-day intervals. This was then BRDF corrected to an apparent view zenith angle of 0° (nadir view) and an apparent SZA of 45°. To obtain seasonal curves of each

vegetation index or band from Modis-MAIAC, we calculated the spatial average for each Modis index or band over the usable area of the two Landsat scenes described above, for each 16d period from Jan 2001 to Sep 2016, then obtained the long-term Modis average for each 16d period. This provided an "expected" ranking of each index to be corroborated by local L8 across the two sets of dates having L8 observations.

To answer Question 2 (What are the possible biological drivers for Modis-MAIAC EVI, NIR and Gcc seasonality?), we obtained 16d spatial averages of EVI and of Gcc in two small windows of 8x11 Modis-MAIAC pixels, one centered on the K34 LBA tower (2.6092°S, 60.2092°W) and one centered on the ATTO tower (2.1433°S, 59.0005°W). Both towers are equipped with Stardot phenocams that monitor leaf demography, based on the fraction of upper canopy crowns that flush new leaves each month [6]. On a monthly basis we separated crown abundances into three post-flush leaf age classes.

Litter production is a proxy for new leaf production in evergreen forest, but only if LAI is stable relative to seasonal litter and new leaf production. We compared monthly litter production from a normal climate year, Sep 2012 to Sep 2013 [15], to local monthly Modis-MAIAC Gcc at the K34 tower region. LAI seasonal change was also calculated following Wu *et al.* [8] as a linear function (y=8.24*x-1.99) of the fraction of crowns that were leafy, the latter derived from phenocams.

3. RESULTS

Our first question (Are L8 seasonal patterns of EVI and of Gcc consistent with BRDF-corrected Modis-MAIAC?) is
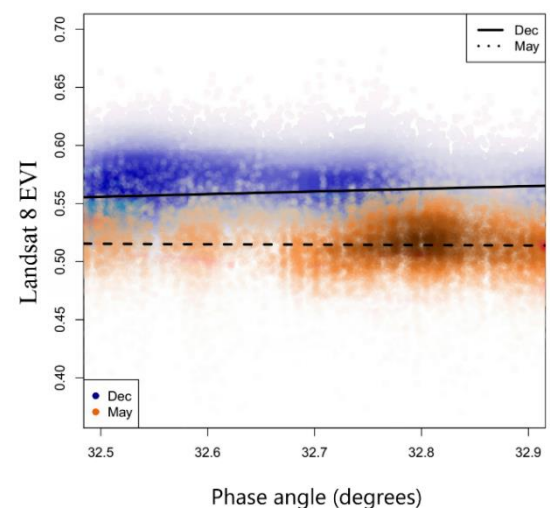
Figure 1. Increase in EVI for Landsat 8 scene 230/61 from May 2015 (brown) to December 2015 (blue); linear fits show that phase angle effect was nil for the chosen Landsat pixels, due to similar solar zenith angles (difference < 0.7°) and near-nadir view angle (< 0.5° off-nadir).

answered in Figures 1 and 2. From May to December, 225 km NE of Manaus, EVI of Landsat 8 increased 8.4% ± 0.13 (Figure 1). Driving this EVI behavior was an increase of 13% ± 0.16 in Landsat NIR reflectance. Local Modis-MAIAC EVI at the ATTO tower which is in this same L8 scene (Figure 3) also peaked in December after a minimum in May, as did MAIAC EVI across the full L8 scene (not shown).

The three L8 images 160 km SSE of Manaus also corroborate the temporal ranking of EVI (not shown) and of Gcc from Modis-MAIAC (Figure 2). Amplitudes of seasonal change were similar fo the two sensors.
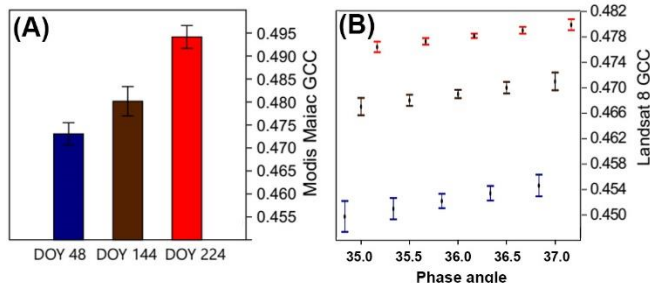
Figure 2. Seasonal Gcc for Modis-MAIAC (A) and Landsat 8 (B) in area of Landsat scene 230/63. Colors blue-brown-red show low-medium-high Gcc ranking for both sensors. Respective dates are 11Feb, 25May, 02Aug. Error bars in B are 95% CI of the mean for each date in each of five narrow phase angle bins.

Our second question (What are the possible biological drivers for Modis-MAIAC EVI, NIR and Gcc seasonality?) is addressed in Figures 3 and 4. At ATTO tower, seasonal Modis-MAIAC Gcc closely followed the abundance of recently flushed upper canopy crowns 0-1 mo age ($R^2 = 0.76$, $p < 0.001$). Seasonal Gcc from Landsat and from Modis-MAIAC in Figure 1 were also consistent with the seasonal abundance of crowns with recently flushed leaves at ATTO.
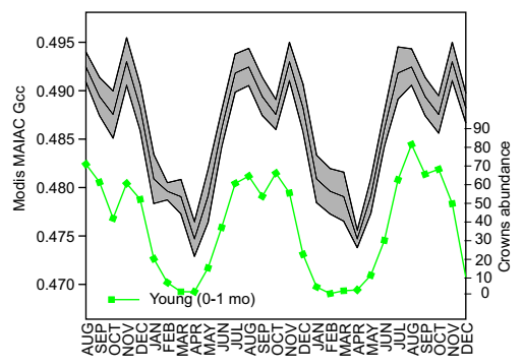

Figure 3 Young leaves (0-1 mo age) and seasonal Modis MAIAC Gcc (95% CI of the mean) from Aug 2013 to Dec 2015 at ATTO site.

At K34 tower, Modis MAIAC Gcc closely tracked litter production ($R^2 = 0.84$, $p < 0.001$), our proxy for new leaves..

LAI was a poor predictor of EVI at ATTO ($R^2 = 0.20$, $p = 0.02$). Total LAI at ATTO was seasonally stable relative to strong changes in leaf age class abundance (Figure 4), justifying our use of strongly seasonal litter production as a proxy for new leaf production at the nearby K34 site.

Seasonal Modis-MAIAC EVI was strongly correlated with the abundance of upper canopy crowns having the 'mature' leaf age class, 2-7 mo age (Figure 4) at ATTO ($R^2 = 0.82$, $p < 0.001$).
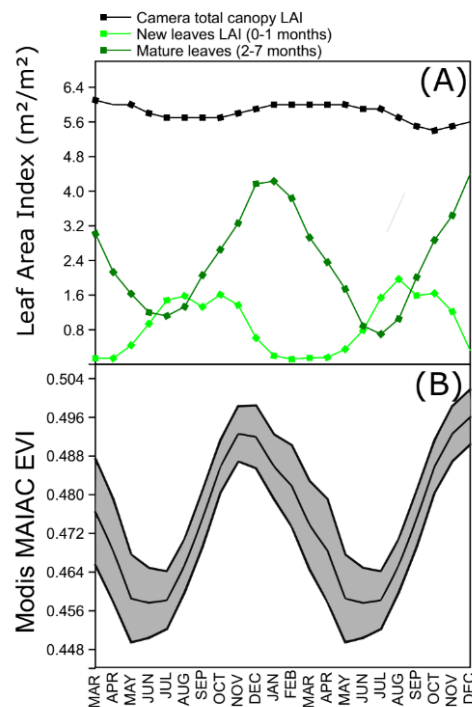
Figure 4. Phenocam-based leaf area index (LAI) and LAI fraction in two age classes, new leaves (0-1 mo) and mature leaves (2-7 mo) for the ATTO site (A); Seasonal Modis MAIAC EVI from March of 2014 to December 2015 at ATTO site (B) closely tracked mature leaf age class in panel A.

4. DISCUSSION

Our results confirm and extend those of Gonçalves *et al.* [9]. With reliable Landsat 8 OLI data – requiring little or no BRDF correction and with high quality cloud masking – we have now extended to two new large areas (two Landsat scenes) in the Central Amazon, confirmation of mid dry season green-up peak for Gcc and late dry season peak for EVI. Furthermore, Landsat 8 provides independent validation of the BRDF inversion of Modis-MAIAC.

Abundance of young leaves drives Modis-MAIAC Gcc signal. This opens a new perspective on leaf phenology and demography patterns detectable with Modis-MAIAC. For example, Modis Gcc seasonality is consistent with RGB tower camera data and with high resolution QuickBird data,

for which Lopes *et al.* [6] found that recently flushed crowns have higher Gcc than other crown phenostages.

Abundance of leaves 2-7 mo old appears to be the biological driver behind the seasonality of EVI. Laboratory spectra of tropical forest leaves of know age also show higher NIR reflectance for mature stage leaves [16, 17]. This study also confirms and extends to a broader geographic area the observations of Lopes *et al.* [6] and Wu *et al.* [7, 8] about leaf age controlling the seasonal EVI signal.

Finally, using both vegetation indices Gcc and EVI from Modis MAIAC as predictors of forest photosynthesis (GPP) may provide more accurate estimates of GPP in evergreen tropical forests where GPP is mainly driven by leaf demography.

5. CONCLUSION

Landsat 8 OLI image sets chosen so that BRDF effects are small to nil corroborate the seasonal signal of BRDF-corrected Modis MAIAC in the Central Amazon, for two vegetation indices: Gcc and EVI. These results do not support the conclusions of Morton et al. [4] of consistent (i.e., constant) EVI greenness throughout the year in Central Amazon forests. Abundance of young and mature leaf age classes drive the seasonal signal of Gcc and EVI, respectively, in Modis MAIAC. LAI has minor importance for explaining seasonal EVI across the Central Amazon.

6. REFERENCES

[1] Huete, A.R., Didan, K., Shimabukuro, Y.E., Ratana, P., Saleska, S.R., Hutyra, L.R., &Myneni, R.B. Amazon rainforests green-up with sunlight in dry season. *Geophysical Research Letters*, 33(6), L06405, (2006).

[2] Restrepo-Coupe, N., Rocha, H.R. da, Hutyra, L.R., Araujo, A.C. da, Borma, L.S., Christoffersen, B.O., … Saleska, S.R. What drives the seasonality of photosynthesis across the Amazon basin? A cross-site analysis of eddy flux tower measurements from the Brasil flux network. *Agricultural and Forest Meteorology*, 182, 128–144, (2013).

[3] Galvão, L.S., Santos, J.R., Roberts, D.A., Breunig, F.M., Toomey, M., Moura,Y.M. On intra-annual EVI variability in the dry season of tropical forest: A case study with MODIS and hyperspectral data. *Remote Sensing of Environment*, 115, 2350-2359, (2011).

[4] Morton, D.C., Nagol, J., Carabajal, C.C., Rosette, J., Palace, M., Cook, B.D., ...North, P.R.J. Amazon forests maintain consistent canopy structure and greenness during the dry season, *Nature*, 506 (7487), 221–224, (2014).

[5] Bi, J., Knyazikhin, Y., Choi, S., Park, T., Barichivich, J., Ciais, P., ... Myneni, R. B. Sun-light mediated seasonality in canopy structure and photosynthetic activity of Amazonian rainforests. *Environmental Research Letters*, 10(6), (2015).

[6] Lopes, A.P., Nelson, B.W., Wu, J., Graça, P.M. L., Tavares, J.V., Prohaska, N., ... Saleska,S.R. Leaf flush drives dry season green-up of the Central Amazon, Remote Sensing of Environment, 182: 90-98, (2016).

[7] Wu, J., Kobayashi, H., Stark, S.C., Meng, R., Guan, K., Tran, N.N., ... & Oliviera, R.C. Biological processes dominate seasonality of remotely sensed canopy greenness in an Amazon evergreen forest. *New Phytologist*. 217(4),1507-1520, (2017)

[8] Wu, J., Albert, L.P., Lopes, A.P., Restrepo-Coupe, N., Hayek, M., Wiedemann, K.T., ... Saleska, S.R. Leaf development and demography explain photosynthetic sea- sonality inAmazon evergreen forests. *Science*, 351(6276), 972–976, (2016).

[9] Gonçalves, N.B., Nelson, B.W., Lopes.A.P.. Scaling up canopy leaf phenology in the Central Amazon – from tower mounted RGB cameras to Landsat 8, *XVIII Simpósio Brasileiro de Sensoriamento Remoto -- SBSR*, (2017).

[10] Maeda, E.E., & Galvão, L.S. Sun-sensor geometry effects on vegetation index anomalies in the Amazon rainforest. *GIScience & Remote Sensing*, 52(3), 332-343, (2015).

[11] Candra, D.S., Phinn, S., and Scarth, P. Cloud and cloud shadow masking using multi-temporal cloud masking algorithm in tropical environmental. *International Archives of the Photogrammetry, Remote Sensing and Spatial Information Sciences*, vol. XLI-B2, 95-100, (2016).

[12] Conrad, O., Bechtel, B., Bock, M., Dietrich, H., Fischer, E., Gerlitz, L., Wehberg, J., Wichmann, V., and Böhner, J. System for Automated Geoscientific Analyses (SAGA) v. 2.1.4, *Geoscientific Model Development*, 8, 1991-2007, (2015).

[13] Valeriano, D.M., Mello, E.M.K., Moreira, J.C., Shimabukuro, Y.E., Duarte, V., Souza, I.M., ... Souza, R.C.M. Monitoring tropical forest from space: the PRODES digital project. *International Archives of Photogrammetry Remote Sensing and Spatial Information Sciences*, 35, 272-274, (2004).

[14] Rennó, C.D., Nobre, A.D., Cuartas, L.A., Soares, J.V., Hodnett, M.G., Tomasella, J., & Waterloo, M.J. HAND, a new terrain descriptor using SRTM-DEM: Mapping terra-firme rainforest environments in Amazonia. *Remote Sensing of Environment*, 112 (9), 3469-3481, (2008).

[15] Ourique, L.K., Silva, R.O., de Souza, C.A.S., Noguchi, H., dos Santos, J., & Higuchi, N. Relationship of litter fall with diameter increment in an old growth forest in central Amazon region. *Scientia Forestalis*, 44(112), 875-886, (2017).

[16] Roberts, D.A., Nelson, B.W., Adams, J.B., & Palmer, F. Spectral changes with leaf aging in Amazon caatinga. *Trees-Structure and Function*, 12(6), 315-325, (1998).

[17] Chavana-Bryant, C., Malhi, Y., Wu, J., Asner, G. P., Anastasiou, A., Enquist, B. J., ... & Martin, R. E. Leaf aging of Amazonian canopy trees as revealed by spectral and physiochemical measurements. *New Phytologist,* 214(3), 1049-1063, (2017).